The 11th International Congress
Motor Vehicles & Motors 2026
Kragujevac, Serbia
October 8th - 9th, 2026

Motor Vehicles & Motors

MVM2026-067
https://doi.org/10.24874/CMVM2026.067
Original scientific paper

**Luka Milić**[1]
**Ilija Vidović**[2]
**Matija Simanić**[3]
**Momir Drakulić**[4]
**Aleksandar Đurić**[5]

# ADDITIVE MANUFACTURING AS A FABRICATION METHOD FOR A LIGHTWEIGHT TRACKED ROBOT PLATFORM

**ABSTRACT:** Additive manufacturing has evolved from a rapid-prototyping niche into a production-grade fabrication method spanning distinct polymer and metal process families, each defined by a different trade-off between accessibility, precision, and mechanical performance. This paper traces that development, from the earliest stereolithography and selective laser sintering patents through material extrusion and metal powder-bed fusion, and examines how these trade-offs translate into a concrete fabrication decision. Fused Deposition Modelling (FDM) using Polylactic Acid (PLA) and Thermoplastic Polyurethane (TPU) was selected for the design and fabrication of a lightweight tracked robot platform, chosen for its low cost, minimal training requirement, and iterative design flexibility despite known limitations in surface resolution and interlayer strength. The resulting platform combines a multipart, dovetail-jointed PLA chassis with a fully 3D-printed drivetrain, a 68-tooth TPU track loop engaging a PLA drive sprocket at a fixed circular pitch, demonstrating that a functional tracked mobility system can be produced entirely by fused deposition modelling, without tooling, from a small number of printed parts. The platform serves as an applied case validating the process and material trade-offs discussed throughout the paper.

**KEYWORDS:** additive manufacturing; fused deposition modelling; material extrusion; PLA; TPU; tracked robot platform

[1] *Luka Milić, University of Defence in Belgrade, Military Academy, Veljka Lukića Kurjaka 33, Belgrade, Serbia, luka.milic777@gmail.com*
[2] *Ilija Vidović, University of Defence in Belgrade, Military Academy, Veljka Lukića Kurjaka 33, Belgrade, Serbia, ilijavidovic50@gmail.com*
[3] *Matija Simanić, University of Defence in Belgrade, Military Academy, Veljka Lukića Kurjaka 33, Belgrade, Serbia, msimanic4@gmail.com*
[4] *Momir Drakulić, University of Defence in Belgrade, Military Academy, Veljka Lukića Kurjaka 33, Belgrade, Serbia, momir.drakulic@va.mod.gov.rs, https://orcid.org/0000-0002-8367-7281*
[5] *Aleksandar Đurić, University of Defence in Belgrade, Military Academy, Veljka Lukića Kurjaka 33, Belgrade, Serbia, aleksandar.djrc@gmail.com, https://orcid.org/0000-0002-2165-528X*

# PRIMENA ADITIVNIH TEHNOLOGIJA U IZRADI LAKOG GUSENIČNOG ROBOTA

**REZIME:** Aditivne tehnologije su se razvile od tehnologije pretežno korišćene za brzu izradu prototipova do proizvodnog metoda izgradnje industrijskog nivoa, koji obuhvata različite porodice procesa zasnovanih na polimerima i metalima, pri čemu svaku karakteriše drugačiji odnos između pristupačnosti, preciznosti i mehaničkih performansi. Ovaj rad prati taj razvoj, počevši od najranijih patenata stereolitografije i selektivnog laserskog sinterovanja, preko ekstruzije materijala do topljenja metalnog praha u sloju, i razmatra kako se ovi kompromisi prevode u konkretnu odluku o načinu izrade. Modelovanje topljenim nanosom (FDM), uz upotrebu polilaktidne kiseline (PLA) i termoplastičnog poliuretana (TPU), izabrana je za projektovanje i izradu lake gusenične robot-platforme, zbog niske cene, minimalnih zahteva za obukom i fleksibilnosti za iterativno projektovanje, uprkos poznatim ograničenjima u pogledu kvaliteta površine i čvrstoće veze između slojeva. Dobijena platforma kombinuje višedelnu šasiju od PLA materijala, spojenu vezom tipa „lastin rep" (dovetail), sa pogonskim sklopom koji je u potpunosti izrađen 3D štampom, gusenicom od TPU materijala sa 68 zubaca koja se uklapa u pogonski lančanik od PLA materijala pri konstantnom koraku. Ovo pokazuje da je funkcionalan gusenični sistem kretanja moguće izraditi isključivo tehnologijom modelovanja topljenim nanosom (FDM), bez alata, od malog broja štampanih delova. Platforma služi kao primenjeni primer koji potvrđuje kompromise u izboru procesa i materijala razmatrane u radu.

**KLJUČNE REČI:** aditivne tehnologije; modelovanje topljenim nanosom (FDM); ekstruzija materijala; PLA; TPU; gusenična robot-platforma

## INTRODUCTION

Modern mechanical engineering depends increasingly on production technologies that allow fast, precise and economical fabrication of technical systems. Conventional subtractive methods, like machining, casting and other related processes, remain the backbone of industrial production, but they struggle to fabricate complex geometries efficiently and offer limited room for rapid design iteration.

Additive manufacturing takes the opposite approach: material is added layer by layer, directly from a digital three-dimensional model, instead of being removed from a solid block. This shifts the constraints of production. Geometric complexity that would be expensive or impossible to machine becomes routine, material waste drops sharply, and, most importantly for early-stage development, a functional prototype can be produced directly from a CAD file within hours rather than weeks.

That last property, rapid prototyping, is the reason additive manufacturing was chosen as the fabrication method for a lightweight tracked robot platform developed as a demonstrator. The platform is not the subject of this paper on its own terms; it is the applied case through which the technology classification and historical development discussed below translate into an actual design decision: material extrusion was selected over the alternative processes precisely because of the trade-offs described in the historical and classification sections below. The chassis design, the resulting material selection, and the design, dimensioning and fabrication of the tracked drive system are addressed in the sections that follow.

Additive manufacturing today spans mechanical, automotive, aerospace, biomedical and robotic engineering, and its role has expanded well beyond producing quick prototypes to include the development of finished, functional parts and production-grade components. Understanding how it reached that position, and how its main process families differ from one another, is a necessary starting point before any discussion of a specific fabrication choice.

## HISTORICAL DEVELOPMENT OF ADDITIVE MANUFACTURING

The origin of additive manufacturing goes back to the early 1980s, when researchers first explored building physical objects layer by layer from digital data. The earliest documented account of this idea comes from the Japanese engineer Hideo Kodama, who in 1981 described a method for building a three-dimensional model by progressively hardening a UV-sensitive photopolymer one layer at a time (Kodama, 1981). Kodama did not secure patent protection in time, and the concept did not reach commercial application at that stage.

The turning point came in the mid-1980s. In 1986, the American engineer Charles Hull patented stereolithography (SLA), a process in which thin layers of photopolymer are cured by a directed ultraviolet light source (Hull, 1986).

Hull co-founded *3D Systems* the same year, the first company in the world dedicated exclusively to the production of 3D printers, and stereolithography became the first commercially available additive manufacturing technology.

Two more foundational processes followed within a few years, each hardening material by a different physical mechanism. In 1989, Carl Deckard, then a student at the University of Texas at Austin, patented Selective Laser Sintering (SLS), in which a laser selectively fuses particles of a powdered material into a solid mass (Deckard, 1989). Around the same time, Scott Crump developed Fused Deposition Modelling (FDM), in which a thermoplastic material is heated to a molten state and deposited layer by layer through a nozzle, filing the founding patent in 1989 (Crump, 1992). Crump and his wife founded *Stratasys*, which brought FDM to market, and after the original patent expired, opened the door to the low-cost desktop 3D printers now common in hobbyist and educational settings.

Through the 1990s and into the early 2000s, additive manufacturing gradually shifted from a tool limited to rapid prototyping toward direct production of functional parts. Metal-focused processes emerged in this period, chiefly Direct Metal Laser Sintering (DMLS) and Selective Laser Melting (SLM), enabling parts to be built from metal powder rather than polymer and opening the way to serious industrial application (Wohlers & Gornet, 2015). This shift in capability was accompanied by a shift in terminology: the industry and research community gradually moved away from the narrower term "Rapid Prototyping" toward the broader "Additive Manufacturing," a usage since formalized by the international standard ISO/ASTM 52900 (ISO/ASTM, 2021).

# CLASSIFICATION AND GENERAL WORKFLOW OF ADDITIVE MANUFACTURING PROCESSES

## *General process workflow*

Regardless of the specific process, every additive manufacturing technology follows the same underlying workflow, building a part layer by layer from a digital model (Godec et al. 2022).

The starting point is a CAD model of the part. Virtually every modern CAD package can export geometry suitable for additive manufacturing, on one condition: the model must be watertight, with no gaps or self-intersecting surfaces in its mesh, or the export that follows will fail to generate a consistent build path.

The watertight model is exported as an STL file, a mesh representation of the surface as a set of triangulated facets, which has become the de facto standard interchange format between CAD software and slicers regardless of the underlying additive process.

The STL file is then processed by slicer software, which cuts it into a stack of horizontal cross-sections of a chosen layer height and generates the machine-readable build path (G-code for material extrusion machines, or an equivalent exposure/scan pattern for laser-based processes) for each layer.

Once the model is sliced and the build path generated, the machine begins physical fabrication. Independent of the underlying technology, the same cycle repeats: one layer is completed, the build platform (or, in some processes, the tool) shifts by the height of that layer, and the cycle repeats until the part is complete. Most additive processes may also call for some form of post-processing, like support removal, cleaning of residual material, sandblasting or heat treatment, once the build finishes. How extensive this post-processing is depends on the technology and material used (Godec et al. 2022).

This shared workflow, from digital model to physical part, is illustrated in Figure 1, and is what separates additive processes from conventional subtractive manufacturing, regardless of how different the individual hardening mechanisms are from one another.

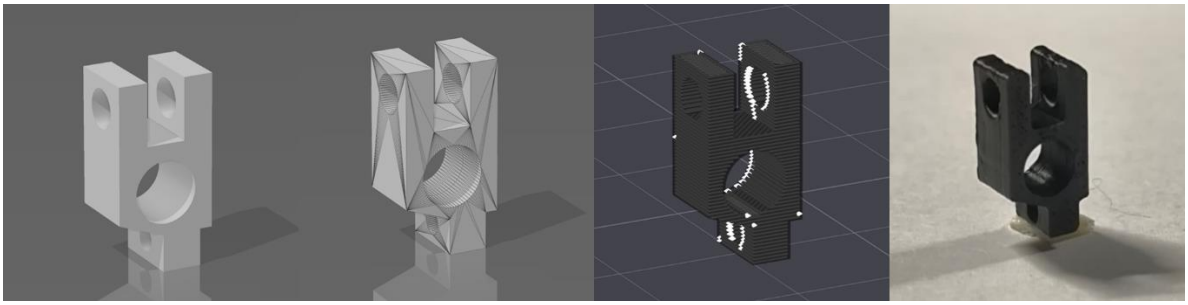


***Figure 1*** The additive manufacturing workflow applied to the track tensioner mount: solid CAD model; triangulated STL mesh export; sliced build path showing the generated toolpath; the finished part after fused deposition modelling

## *Classification of additive manufacturing processes*

Despite a large number of commercial names and patented variants, additive processes can be grouped into a small number of categories based on the physical state of the feedstock and the mechanism used to consolidate it into a solid part. Four process families account for the large majority of current use: SLA, SLS, FDM and SLM/DMLS.

**Photopolymer- and powder-based polymer processes (SLA and SLS)**

Stereolithography (SLA) belongs to the category of processes in which a liquid photopolymer is selectively cured by directed light, most commonly a UV laser. The light source traces the cross-section of the current layer across the resin surface, causing local curing, after which the platform shifts by one layer height and a new liquid layer flows over the cured surface (Kodama, 1981; Hull, 1986). The cycle repeats until the part is complete.

Selective Laser Sintering (SLS) follows the same principle of layer-by-layer selective consolidation by a scanning laser, applied to a different feedstock state. A powdered material, spread in a thin layer across the build area, is struck by a laser that selectively heats and fuses (sinters) the particles exactly along the cross-section of the current layer (Deckard, 1989).

**Material extrusion (FDM)**

Fused Deposition Modelling (FDM) is based on extruding a thermoplastic filament, heated to its melting point and forced through a small nozzle that moves along the path defined by the cross-section of the current layer, depositing molten material onto the previously built layer, where it cools and solidifies (Crump, 1992).

FDM spans a wide material range for a single process. Common thermoplastics such as PLA, ABS and PETG cover general-purpose and educational use. Engineering-grade materials such as polyamide, polycarbonate and fiber-reinforced composites extend the process into higher strength and temperature applications. Flexible filaments such as TPU behave closer to rubber than to a rigid plastic, extending FDM into parts that need to bend or absorb impact rather than hold a fixed shape.

No other additive process has reached the accessibility of FDM. Where SLA and SLS require expensive, controlled build environments, FDM machines and materials are comparatively inexpensive, require no laser, no powder handling and no UV source, and the training needed for routine operation is minimal. Finished parts are, aside from any support removal, immediately usable, without the chemical post-curing SLA requires or the powder-recovery process SLS requires (Godec et al. 2022). Because switching between designs on an FDM machine is simply a matter of loading a new file, the process is particularly well suited to rapid prototyping and small production runs, where the geometry is expected to change across several design iterations before it is finalized.

That accessibility comes at a cost. FDM parts are mechanically anisotropic, meaning that the bond between printed layers is consistently weaker than the material itself, so a part is markedly weaker when loaded across layers than along them. Another limitation is surface resolution, limited on two independent axes: vertically, by the chosen layer height, which produces a visible stepped effect on curved surfaces regardless of print quality, and horizontally, by the nozzle diameter, which sets a hard lower bound on wall thickness and feature size that no amount of slicer tuning can overcome (Godec et al. 2022). For context, SLA achieves markedly finer surface detail, since its resolution is set by the width of the light source rather than a physical nozzle, and SLS achieves more isotropic mechanical properties without the pronounced interlayer weakness that characterizes FDM.

The trade-off is consistent across the comparison: FDM exchanges precision and mechanical isotropy for cost, simplicity and accessibility, which is exactly the exchange that favours it during the prototyping stage of product development, and exactly the exchange that stops favouring it once a part must carry a real structural or thermal load in service.

**Metal powder-bed fusion (SLM/DMLS)**

There is a point beyond which no thermoplastic, reinforced or not, can meet a part's requirements, whether because of temperature exceeding what a polymer can tolerate, a load that the anisotropy of a layered polymer structure would make risky to carry, or simply a functional need for the part to be metal.

At that point, additive manufacturing shifts from polymer to metal, and with that shift comes an entirely different set of technical requirements. Molten metal, unlike molten thermoplastic, has very low viscosity, which in turn means it behaves more like water than a thick paste, and cannot be extruded through a nozzle while holding a precise layer geometry.

For this reason, SLM and DMLS machines do not deposit molten metal at all. Instead, a thin layer of metal powder is selectively melted, point by point, by a laser, and solidifies as the laser moves on to the next location (Ponnusamy et al., 2020). Because metal particles at high temperature react readily with oxygen, the entire process takes place inside a chamber filled with inert gas, typically nitrogen or argon, preventing oxidation during the build.

SLM and DMLS are frequently used as synonyms, though a technical distinction exists between them: DMLS, a term originally introduced by EOS, denotes partial sintering, particles bond at the molecular level without complete melting, which is best suited to multi-component alloys, while SLM denotes complete melting into a homogeneous mass, suited to pure metals. In current practice, most machines achieve full melting regardless of the manufacturer's chosen name, making the distinction largely historical (Ponnusamy et al. 2020).

Commonly used metal powders include stainless steels, titanium alloys, aluminium alloys and nickel superalloys, selected according to the specific requirement of the application, like titanium for its strength-to-weight ratio or nickel superalloys for resistance to extreme temperature (Tuli et al. 2024).

Once the metal is fully melted, the resulting parts reach approximately 99% density, with mechanical properties comparable to a wrought part of the same composition (Ponnusamy et al., 2020), a fundamental departure from FDM, where interlayer anisotropy remains a permanent limitation regardless of process parameters. This combination of full geometric freedom, which allows for internal channels, lattice structures, topology-optimized forms, and forged-equivalent material quality is why SLM and DMLS are established in biomedical implants tailored to patient-specific anatomy, and in the aerospace and automotive industries (Ponnusamy et al. 2020).

Comparing FDM against metal powder-bed fusion is most useful not in terms of cost or mechanical properties directly, but in terms of the role each plays in product development. FDM is the technology of rapid materialization: hours, not days or weeks, separate a digital model from a physical prototype, which lets design decisions be tested physically before significant resources are committed, catches errors early, and keeps the cost of each design iteration low. In that phase, where the goal is to verify form, fit and concept, anisotropy and limited strength are an acceptable trade for the speed and accessibility FDM offers. Metal additive technologies enter the picture once a prototype needs to become a functional, service-reliable part, at which point the geometric freedom additive manufacturing offers becomes valuable precisely in combination with mechanical properties comparable to wrought metal (Ponnusamy et al., 2020). That is the point in development where the cost and complexity of the metal process become justified, because the alternative is conventional manufacturing with all of its own constraints on geometric freedom. The two technologies are, in that sense, not competitors but two steps along the same development path.

## APPLICATION CONTEXT: FROM INDUSTRIAL PRODUCTION TO FIELD LOGISTICS

The capability to produce a finished, service-reliable metal part without tooling or a long production chain has found application across a wide range of industries. Two examples illustrate this shift: one from automotive manufacturing, the other from military field logistics.

In the automotive industry, metal additive manufacturing has moved beyond prototyping into structural, production-grade components. The clearest example is the *Czinger 21C hypercar*, built by *Czinger Vehicles* in partnership with *Divergent 3D*, whose chassis nodes and rear subframe are generatively designed by AI and then produced directly by metal powder-bed fusion in aluminium alloys, replacing the tooling, casting and stamping steps of conventional vehicle manufacturing entirely (Kerns, 2021). This combination of generative design and metal AM is the automotive-scale expression of the same geometric freedom discussed above in the context of biomedical and aerospace applications.

At the 2024 NATO exercise *Steadfast Defender*, the largest NATO exercise in Europe since the Cold War, the British Army used mobile 3D printers to fabricate spare parts directly in the field for the first time, under a program known as *Project Brokkr*, replacing the standard procedure of waiting for a replacement part to arrive from a depot (UK Ministry of Defence, 2024). This approach directly reduces dependence on long, costly supply chains, and gains particular significance for older vehicles whose parts are no longer available from the original manufacturer.

## CHASSIS DESIGN AND FABRICATION

The robot chassis is the geometrically most complex single component in the platform (Figure 2), since it must simultaneously house the power and drive electronics, carry the loads transmitted by the torsion-spring suspension, the drive motor, and the track tensioning mechanism, and do so within two fixed physical constraints: the minimum

volume required by the components themselves, and the maximum build volume of the 3D printer, 180 mm along each axis.

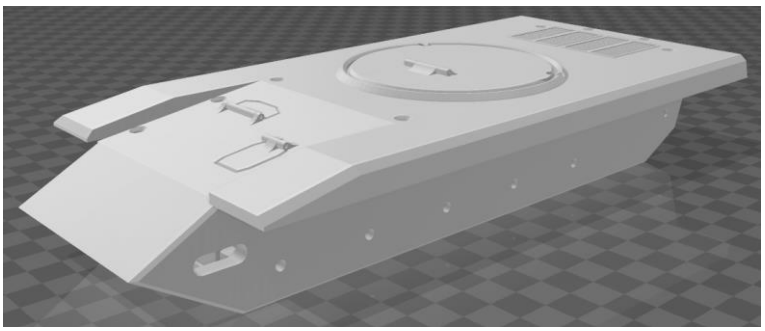


***Figure 2*** Model of platform's chassis

## *Material Choice*

PLA was selected as the chassis material for two reasons directly tied to the constraints above. First, the component carries structural loads rather than needing to flex, so PLA's characteristic stiffness and brittleness, a limitation for the flexible track components discussed below, is an advantage here rather than a drawback. Second, PLA's low coefficient of thermal expansion limits shrinkage and warping during cooling, which is what makes the dovetail joint between the two printed halves viable at all: a material more prone to warping would introduce enough dimensional drift at the joint face to compromise the fit the slicer's automated dovetail profile depends on.

## *Spatial Constraints and Sectioning*

The chassis body exceeds the printer's build volume on its own, with a total length of 230 mm. Rather than redesigning the geometry to fit within a single print, the body was split into two separate sections using the printer software's built-in model-cutting function, which generates a dovetail-profile joint at the cut automatically. The chassis lid was split the same way and for the same reason, giving the assembled chassis four printed sections in total. This gives each pair of halves a mechanically positioned connection without any additional fasteners, and the decision to leave the joints unengineered in the CAD model itself, relying on the slicer to resolve them, was made deliberately: defining fit tolerances at the design stage would have added time without a corresponding benefit, since the automated dovetail already provides adequate mechanical registration between each pair of halves.

## *Anisotrophy as a Design Parameter*

FDM's characteristic anisotropy, discussed above as a general limitation of the process, was treated as a design parameter rather than an obstacle in three specific areas of the chassis. In the zones where the torsion springs introduce concentrated loads into the body, a local print-parameter override was used to increase wall count and infill density only within that region, without affecting the print settings of the rest of the part, raising local strength exactly where the layer-to-layer bond would otherwise be the weakest point in the structure, without adding unnecessary mass or print time elsewhere. The axle bushings and the track tensioner mount were oriented so that the working load acts along the plane of the printed layers, the strongest loading direction for an FDM part, while the precision bores for the axles were oriented perpendicular to the print plane, where FDM achieves its highest geometric accuracy.

# DRIVETRAIN DESIGN AND FABRICATION

Following the fabrication of the robot chassis and the definition of the centre distance between the drive sprocket and the idler wheel, the design of the drivetrain proper begins.

## *Concept Selection*

A continuous flexible track loop was selected over a conventional articulated segmented track. The primary motivation stems from the fact that the robot is fabricated by 3D printing: producing a functional articulated track at this scale would require printing a large number of miniature components, intricate assembly, and the insertion of metallic or plastic pins, increasing the risk of mechanical failure and complicating maintenance on a small-scale platform.

The continuous-loop approach instead allows the entire flexible element of the drive system to be manufactured in a single printing process using TPU, yielding a homogeneous structure. This eliminates mechanical joints, the points where friction and accelerated wear typically occur in a segmented track, extending the track's operational lifespan, and is significantly faster to manufacture, since the loop is produced as a single continuous body with integrated driving teeth for positive engagement with the drive sprocket. This also contributes to a reduction in the platform's overall mass.

## *Geometric Dimensioning of the Drive Sprocket*

The chassis design imposed a strict spatial constraint, limiting the maximum outer diameter of the drive sprocket to 20 mm. All other transmission parameters, the sprocket's pitch diameter, tooth height, and track pitch, were derived from this primary constraint.

The drive sprocket was fabricated from PLA at 100% infill, chosen for its high strength, which improves durability under load despite the stress concentration inherent to gear teeth, and resists tooth wear over extended operation.

Standard theoretical gearing formulas served only as an initial baseline, since they assume a rigid mechanical element; the final geometry was established empirically through iterative printing, testing, and refinement. Engagement between the rigid sprocket and the printed track loop is governed by the circular pitch, the arc distance between adjacent tooth axes measured along the sprocket's pitch circle. The initial theoretical tooth root thickness of 3.556 mm produced excessive friction and mechanical binding when rounding curves, caused by the flexibility of the TPU track and microscopic filament bleed during printing, and was empirically reduced to 3 mm, which allowed smooth engagement at rotational speeds up to 200 rpm. The tooth itself was given a height of 2 mm and a top face width of 2 mm, with a slightly tapered trapezoidal profile at a 20° pressure angle, the standard engineering compromise between tangential and radial force, which here also lets the tooth enter and exit the track aperture at an angle without binding or deforming the track material.

Based on these derived and empirically adjusted parameters, the drive sprocket was modelled in CATIA (Figure 3), annotated with the dimensions used to generate the printing G-code.

A separate alignment problem emerged from the drive motor's output shaft, which proved too short to bring the sprocket into the same lateral plane as the idler and road wheels, causing the track to twist across its width during rotation instead of running flat. This was resolved by extending the rear face of the sprocket with an adjustable mounting boss, bringing the sprocket back into alignment with the rest of the drivetrain without requiring a longer motor shaft or a redesign of the wheel train itself (Figure 4).

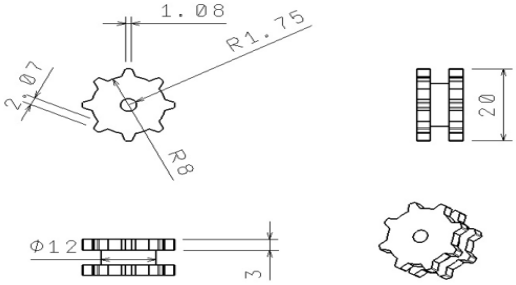



***Figure 3*** Model of the drive sprocket



***Figure 4*** Finished drive sprocket with added mount

## *Geometric Dimensioning of the Continuous Track*

The track loop was fabricated from TPU as a continuous closed ring with internal gearing, chosen so the highly deformable, elastic loop could install directly onto the chassis and conform to the geometry of the wheels and guide elements without a separate assembly step.

*Track pitch.* Continuous power transmission at operating speeds up to 200 rpm without binding or destructive friction requires the pitch of the track's internal apertures to match the circular pitch calculated on the sprocket's pitch circle exactly.

*Track cavity, thickness, and profile.* Unlike the sprocket, where tooth thickness was empirically reduced to 3.0 mm, the track's apertures had to remain dimensioned to allow that same tooth to enter and exit freely along curved paths. As the TPU loop negotiates the drivetrain's 20 mm bend radius, it deforms and contracts slightly along its inner circumference; against the theoretical tooth root width of 3.556 mm, a functional backlash clearance of 0.556 mm was provided for smooth engagement. The internal drive teeth on the track are 2 mm high, the base track thickness

is 4 mm, sufficient to resist elongation and disengagement during motion, and a 4 mm guiding ridge works with the road wheels to further reduce the risk of track derailment.

*Track length and segment count.* The number of teeth must be an integer for the loop to close into a continuous ring without a pitch discontinuity; the calculation yielded 68 internal cavities, and prototype testing confirmed this segment count, combined with the elastic deformability of the TPU, produces optimal tensioning across the chassis frame. Total track length was determined from the perimeter of the triangle formed by the idler, support, and drive wheels, giving a maximum usable length of 478 mm and a minimum of 465 mm; the tensioning system's axial movement of the idler wheel accommodates this range.

*CAD modelling in CATIA.* The track loop was modelled to maintain a constant pitch of 6.89 mm around its full perimeter, with the pitch circle diameter derived from the target total loop length. A construction circle of 149.14 mm diameter was defined in the Sketcher workbench to represent the track's neutral kinematic axis, and the cross-sectional profile of a single tooth was defined within its corresponding 5.29° angular sector. A circular pattern replicated this segment 68 times around the central axis; because the pitch circle diameter was mathematically exact, the final segment closed seamlessly into the first, producing a continuous, internally geared ring without pitch error or geometric discontinuity (Figure 5). The finished track loop, printed in TPU, is shown in Figure 6.

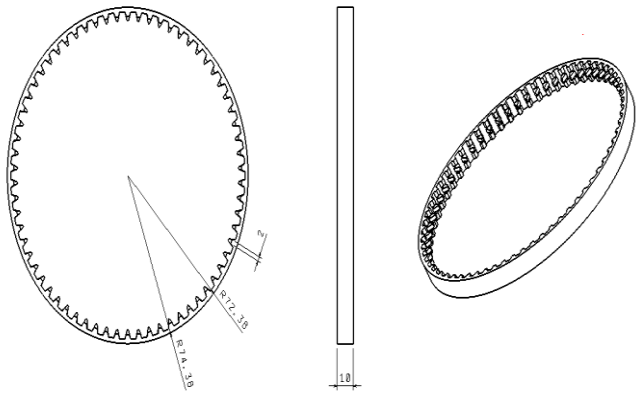



***Figure 5*** Model of the circular ring with internal gearing



***Figure 6*** The completed TPU track loop after printing

## *MATERIAL SELECTION FOR THE DRIVETRAIN*

The development of modern unmanned ground platforms and lightweight military robots requires materials that balance structural strength, ductility, resistance to environmental factors, and minimal self-mass. A hybrid concept combining two thermoplastic polymers, Polylactic Acid (PLA) and Thermoplastic Polyurethane (TPU), was selected for the rigid structural elements and flexible components of the drive system respectively (Demirtas et al. 2023).

### PLA: Structural Components

The dimensional stability behind the chassis' dovetail joint, discussed above, follows from PLA's specific thermal behaviour: a glass transition temperature between 55 °C and 65 °C, a melting point between 150 °C and 180 °C, and a low coefficient of thermal expansion that results in minimal shrinkage during cooling and limits warping at the corners of a printed part (Demirtas et al. 2023).

The mechanical properties of printed PLA components are anisotropic and depend directly on layer orientation, extrusion temperature, and infill density. An optimally printed PLA component is characterized by a tensile strength between 50 MPa and 70 MPa, comparable to certain cast aluminium alloys under static stress; a Young's modulus between 3 GPa and 3.5 GPa, which imparts significant stiffness and resists shaft deflection under track tension; and high compressive strength, though the material remains brittle, with elongation at break of only 2–6%.

### TPU: Flexible Track Components

For continuous track loops and road wheel rings, which are constantly subjected to dynamic fatigue, repetitive bending, and terrain abrasion, high elasticity, shock-absorption capacity, and durability are essential, requirements PLA cannot meet but which TPU fulfils directly. TPU is a linear segmented block copolymer of alternating soft and hard segments, with hardness measured on the Shore scale; TPU 95A, or the slightly softer TPU 85A, is most commonly used for mobile robot tracks (Demirtas et al. 2023).

TPU 95A exhibits elongation at break exceeding 400%, with high elastic recovery, allowing track segments to articulate over small-diameter drive sprockets and tension idlers without cracking or strain-fatigue failure. As a polymer, it also shows exceptionally low abrasive wear against sand, damp soil, and gravel, making it considerably more durable than conventional natural rubber under similar operating conditions. Its high mechanical energy absorption further attenuates dynamic impacts from ground irregularities within the material itself, preventing shock transmission to the rigid PLA wheels and chassis frame (Jayswal et al. 2022).

# CONCLUSIONS

Additive manufacturing has moved from a rapid-prototyping niche into a production-grade fabrication method spanning polymer and metal processes, each defined by a distinct trade-off between accessibility, precision, and mechanical performance. Among these, material extrusion offers the combination of low cost, minimal training requirement, and design flexibility that makes it the appropriate choice for early-stage development of small robotic platforms, despite its inherent limitations in surface resolution and interlayer strength.

This trade-off was validated in practice through the design and fabrication of a lightweight tracked robot platform. PLA was selected for the structural chassis and drive sprocket, where its stiffness and dimensional stability under cooling supported a two-part, dovetail-jointed chassis design and a wear-resistant drive wheel, while TPU was selected for the continuous track loop, where its high elongation at break and elastic recovery allowed a single-piece, internally geared ring to articulate over a small-diameter sprocket without cracking or fatigue failure. The resulting drivetrain, a 68-tooth TPU track loop engaging a 20 mm PLA sprocket at a fixed circular pitch, demonstrates that a fully 3D-printed tracked mobility system, requiring no tooling and assembled from a small number of printed parts, is a viable approach for rapid, low-cost development of small mobile platforms.

Taken together, the process and material trade-offs discussed in the historical and classification sections of this paper translate directly into the design decisions behind the chassis and drivetrain, and the resulting prototype serves as a concrete demonstration that FDM, despite sitting at the accessible end of the additive manufacturing spectrum, is capable of producing a complete, functional mobility platform (Figure 7).

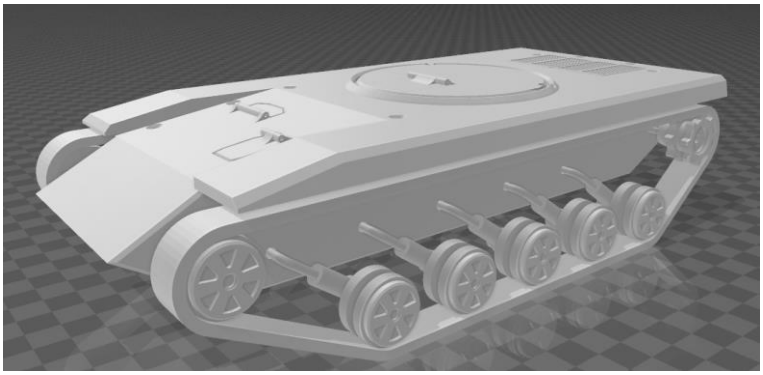


***Figure 7*** Model of completed platform

# ACKNOWLEDGMENTS

This work was supported by the Ministry of Defence, Serbia, under the project „Modelling of Automotive Vehicle Assemblies for the Optimization of Dynamic Parameters”, No. VA-TT/1/26-28.

# REFERENCES

Crump, S. (1992). Apparatus and method for creating three-dimensional objects (U.S. Patent No. 5,121,329).

Deckard, C. R. (1989). Method and apparatus for producing parts by selective sintering (U.S. Patent No. 4,863,538).

Demirtas, B., Sevim, C. & Demirbas, M. D. (2026). Composition-dependent mechanical and thermal behavior of TPU-modified PLA and ABS filaments for FDM applications. *Polymers*, 18(8), 949. https://doi.org/10.3390/polym18080949

Godec, D., Pilipović, A., & Breški, T. (2022). General process workflow in additive manufacturing. In D. Godec et al. (Eds.), A guide to additive manufacturing (pp. 45–57). Springer International Publishing. https://doi.org/10.1007/978-3-031-05863-9_2

Hull, C. W. (1986). Apparatus for production of three-dimensional objects by stereolithography (U.S. Patent No. 4,575,330).

International Organization for Standardization/ASTM International. (2021). Additive manufacturing — General principles — Fundamentals and vocabulary (ISO/ASTM 52900:2021).

Jayswal, A., Liu, J., Harris, G., & Mailen, R. (2023). Creep behavior of 3D printed polymer composites. *Polymer Engineering & Science*, 63(11), 3519-3918. https://doi.org/10.1002/pen.26486

Kerns, J. (2021). Metal 3D printing in automotive: How the Czinger 21C is redefining next-generation car manufacturing. Metal AM Magazine, 7(4). https://www.metal-am.com/articles/metal-3d-printing-in-automotive-how-the-czinger-21c-is-redefining-next-generation-car-manufacturing/

Kodama, H. (1981). Automatic method for fabricating a three-dimensional plastic model with photo-hardening polymer. *Review of Scientific Instruments*, 52(11), 1770–1773. https://doi.org/10.1063/1.1136492

Ponnusamy, P., Rahman Rashid, R. A., Masood, S. H., Ruan, D., & Palanisamy, S. (2020). Mechanical properties of SLM-printed aluminium alloys: A review. *Materials*, 13(19), 4301. https://doi.org/10.3390/ma13194301

Tuli, N. T., Khatun, S., & Rashid, A. B. (2024). Unlocking the future of precision manufacturing: A comprehensive exploration of 3D printing with fiber-reinforced composites in aerospace, automotive, medical, and consumer industries. *Heliyon*, 10(5), e27328. https://doi.org/10.1016/j.heliyon.2024.e27328

UK Ministry of Defence. (2024). World-leading 3D printer used by British Army in the field for first time. GOV.UK. https://www.gov.uk/government/news/world-leading-3d-printer-used-by-british-army-in-the-field-for-first-time

Wohlers, T., & Gorne, T. (2015). *History of additive manufacturing*. https://wohlersassociates.com/wp-content/uploads/2022/08/history2015.pdf